Biochemical Pharmacology, Vol. 38, No. 16, pp. 2621–2630, 1989.
Printed in Great Britain.

0006-2952/89 $3.00 + 0.00

IN VITRO DRUG METABOLISM AND PHARMACOKINETICS OF DIAZEPAM IN CYNOMOLGUS MONKEY HEPATOCYTES DURING CULTURE FOR SIX DAYS

TOM SEDDON, GRAHAM F. LOCKWOOD and RICHARD J. CHENERY*
Smith, Kline & French Ltd, The Frythe, Welwyn, Hertfordshire, U.K.

(*Received* 19 *September* 1988; *accepted* 24 *February* 1989)

Abstract—Diazepam (DZ), *N*-desmethyl diazepam (NOR) and temazepam (TEM) were used as substrates in drug metabolism studies to characterize the changes in cytochrome P-450 mono-oxygenase pathways in hepatocytes isolated from cynomolgus monkeys, during culture for 6 days. Hepatocytes were incubated with DZ (20 μM), NOR (6 μM) or TEM (20 μM) for 3 hr at 3, 24, 48, 96 and 144 hr post-isolation in culture, and the profiles of disappearance of DZ, as substrate, and appearance of its metabolites determined. Major metabolites were NOR, TEM and oxazepam (OX). The kinetic profiles for the disappearance of DZ and the accumulation of metabolite were analysed using a four-compartment model and constants for the rates of formation of the metabolites were derived. There were significant changes during the period in culture for the rate constants of DZ demethylation, but no alteration in the 3-hydroxylation activities. Rates of DZ metabolism were unchanged during the initial 2 days in culture and well maintained for the subsequent 4 days, despite a fall in total cytochrome P-450 to 23% of initial values after 6 days. Cynomolgus monkey hepatocytes produce similar metabolite profiles for DZ to those found in man, both *in vitro* and *in vivo*, indicating that cynomolgus monkey hepatocytes may represent a relatively stable and valuable model of human drug metabolism.

It has been reported that total cytochrome P-450 content declines rapidly in cultures of rat hepatocytes, and typically reduces to less than 30% of the initial values within 48 hr [1, 2]. Concomitant with this decline, there is usually a substantial reduction in many of the mono-oxygenase drug metabolising activities of the hepatocytes [3, 4]. In addition, the metabolizing profiles obtained for xenobiotics in the rat are frequently very different to those obtained in man, reducing the utility of the rat as a model of human metabolism. These observations indicate that for many drugs rat hepatocytes represent a poor *in vitro* model in which to investigate drug metabolizing activities.

Several reports describe methods by which rat hepatocytes can be maintained for longer periods in culture, by additions of hormones and/or inducers to the media to reduce losses in cytochrome P-450 enzymes [5–8], and well maintained protein secretion [9, 10], but only rarely have hepatocytes from other species been compared to those of the rat in an effort to establish a more appropriate *in vitro* model of drug metabolism, combining higher stability with a better approximation of human metabolism.

The similarities between human and monkey metabolism *in vivo* indicate that cynomolgus monkey hepatocytes may be valuable as a system in which to model human hepatic drug metabolism. Therefore, studies detailed here were undertaken to characterize the changes *in vitro* in cellular morphology, cytochrome P-450 and drug metabolizing activity of cynomolgus monkey hepatocytes maintained in culture for 6 days.

Coutinho *et al.* [11] described the tissue distribution in cynomolgus monkeys of DZ; a benzodiazepine, effective in the symptomatic relief of anxiety and as a muscle relaxant. They found that DZ was rapidly metabolized to *N*-desmethyl diazepam (NOR), temazepam (TEM) and oxazepam (OX) and that the profiles of DZ and its metabolites in monkey blood were similar to those previously described in human plasma [12, 13].

DZ is metabolized by several pathways, shown in Fig. 1, that are common to several species. It has been shown to be sensitive as a probe of the differences in drug metabolizing activities between rat, rabbit, dog, guinea pig and man *in vitro* [14], and has often been used for kinetic studies *in vivo* in several species, including man [15, 16], dogs [17], rats and mice [16].

In these studies DZ was used as a probe substrate of the cytochrome P-450 mono-oxygenase system, and a compartmental model was developed to describe the changes in the kinetics of the metabolizing pathways of DZ in monkey hepatocytes.

MATERIALS AND METHODS

Materials. 4-(2-Hydroxyethyl)-1-piperazine-ethane sulphonic acid (HEPES), ethyleneglycolbis-(β-aminoethyl ether)- *N,N,N',N'*-tetraacetic acid (EGTA), bovine pancreatic insulin, bovine serum albumin (BSA fraction V), hydrocortisone hemisuccinate and newborn calf serum (mycoplasma and virus screened) were obtained from Sigma Chemical Co. (Poole, U.K.). Earle's balanced salt solution (EBSS; 10× concentrate, calcium and magnesium free, without bicarbonate), sodium bicarbonate solution (7.5% w/v), penicillin (5000 I.U/ml) plus strep-

* Author to whom correspondence should be addressed.

determined after HPLC separation using a Hewlett–Packard 1090A chromatograph fitted with a filter photometric detector (230 nm) and auto-injector. The separation was performed on a Waters C-18 μBondapak 30 cm × 4.6 cm column with pre-frit filter, employing a gradient; methanol (65–78%, v/v) and ammonium acetate (0.01 M, pH 6.00, adjusted with CF_3COOH) (35–22%, v/v), at 1 ml/min. Oven temperature was held at 50° and retention time for DZ as the least polar compound was 9.5 min. The system was controlled by a Hewlett–Packard-85 microcomputer running resident Hewlett–Packard-HPLC software, hard disc and flexible disc as methods cache and recorded with a Hewlett–Packard 3392A integrator.

Authentic standards of DZ, NOR, TEM, OX, 4′-OH DZ and 4′-OH NOR were made-up in water and determined in the same manner as WME samples. External standard curves were constructed, from peak area integration of 5 μl (100 pmol) to 25 μl (500 pmol) injections each of the standard solutions of DZ, NOR, TEM, 4′-OH DZ and 4′-OH NOR. Sample to noise ratio was less than 5% of the lowest standard. Incubated samples were analysed with 14 days of experimentation; metabolites were stable at −80° in WME for at least 90 days.

Analysis of data. A model was developed, based on the scheme in Fig. 1, for the metabolism of DZ in cynomolgus monkey hyepatocytes using prior information about the major routes of DZ metabolism in this species. The assumptions of the model were:

(1) all transfer processes were operating under linear conditions;
(2) the intracellular/extracellular distributions of DZ and its metabolites rapidly attained equilibrium, and were not rate limiting to metabolism;
(3) extracellular administration of metabolites of DZ resulted in an identical pattern of distribution of the metabolites formed intracellularly;
(4) since no information was available about the cellular volumes or intracellular concentrations, all estimated parameters were based on media concentrations.

The disappearance from, or appearance into, the culture media of DZ or its metabolites was followed over 3 hr. In this way data describing eight processes were obtained. These processes were:

(1) the disappearance of DZ following DZ administration;
(2) the appearance and subsequent disappearance of NOR following DZ administration;
(3) the appearance and subsequent disappearance of TEM following DZ administration;
(4) the appearance and subsequent disappearance of OX following DZ administration;
(5) the disappearance of NOR following NOR administration;
(6) the appearance and subsequent disappearance of OX following NOR administration;
(7) the disappearance of TEM following TEM administration;
(8) the appearance and subsequent disappearance of OX following TEM administration.

Mathematical expressions for each of these functions based on the scheme presented in Fig. 1 are given in Appendix 1. Estimates of the model parameters were obtained by simultaneously fitting equations (1)–(8) to the measured media concentrations of parent substrate and metabolites, using the non-linear least squares regression program NONLIN-84, resident on a VAX 11/780, running a VMS operating system. All data points were weighted according to the reciprocal of the observed concentration, and the goodness of fit and adequacy of the model to describe the data was assessed by examination of the residual plots for each function.

RESULTS

Cellular morphology

Hepatocytes were cultured onto collagen-coated plastic six-well plates, maintained in medium buffered with sodium bicarbonate, and were adherent within 30 min, forming regular, tesselated monolayers within 3 hr. The monolayer cells were granular in appearance, with a majority of cells containing single nuclei, but only one nucleolus. Compared with rat hepatocytes, which are adherent within 2 hr, but rarely form monolayers within 5 hr, the monkey hepatocytes showed unusually rapid culturing characteristics.

The morphology of the cells was very well maintained for the whole culture period. The monolayers were initially composed of regular chords of flattened polygonal cells, and during culture the cells retained this polygonal form, with only small changes in the monolayer organisation.

No cells were observed with two nucleoli, whereas rat, dog and guinea pig cells often contained nuclei with two nucleoli, and occasionally three. About 31% of cells were binucleate, compared with rat cells in which between 26% and 32% are binucleate, and dog cells in which about 27% are binucleate.

Cellular cytochrome P-450

Table 1 compares the total cytochrome P-450 content in dog, rat, cynomolgus monkey and human in fresh (3 hr) hepatocyte cultures. Initial levels of total cytochrome P-450 in monkey hepatocytes were found to be high compared with other species. The rate of depletion of total cellular cytochrome P-450, shown in Fig. 2, was lower than that found in rat hepatocytes, so that at 6 days in culture at least 23% of total cytochrome P-450 remained in the cells,

Table 1. Comparison of the total cytochrome P-450 content of hepatocytes isolated from dog, rat, human and monkey liver, cultured for 3 hr in WME, supplemented with hydrocortisone and insulin

Species	Number of preparations	Cytochrome P-450 (pmol/10^6 hepatocytes)
Dog	4	184.3 ± 23.5
Rat	6	257.6 ± 37.3
Human	4	140.1 ± 45.7
Cynomolgus	2	430.2*

Results are given as mean ± SD.
* Mean of two determinations.

determined after HPLC separation using a Hewlett–Packard 1090A chromatograph fitted with a filter photometric detector (230 nm) and auto-injector. The separation was performed on a Waters C-18 μBondapak 30 cm × 4.6 cm column with pre-frit filter, employing a gradient; methanol (65–78%, v/v) and ammonium acetate (0.01 M, pH 6.00, adjusted with CF_3COOH) (35–22%, v/v), at 1 ml/min. Oven temperature was held at 50° and retention time for DZ as the least polar compound was 9.5 min. The system was controlled by a Hewlett–Packard-85 microcomputer running resident Hewlett–Packard-HPLC software, hard disc and flexible disc as methods cache and recorded with a Hewlett–Packard 3392A integrator.

Authentic standards of DZ, NOR, TEM, OX, 4′-OH DZ and 4′-OH NOR were made-up in water and determined in the same manner as WME samples. External standard curves were constructed, from peak area integration of 5 μl (100 pmol) to 25 μl (500 pmol) injections each of the standard solutions of DZ, NOR, TEM, 4′-OH DZ and 4′-OH NOR. Sample to noise ratio was less than 5% of the lowest standard. Incubated samples were analysed with 14 days of experimentation; metabolites were stable at −80° in WME for at least 90 days.

Analysis of data. A model was developed, based on the scheme in Fig. 1, for the metabolism of DZ in cynomolgus monkey hyepatocytes using prior information about the major routes of DZ metabolism in this species. The assumptions of the model were:

(1) all transfer processes were operating under linear conditions;
(2) the intracellular/extracellular distributions of DZ and its metabolites rapidly attained equilibrium, and were not rate limiting to metabolism;
(3) extracellular administration of metabolites of DZ resulted in an identical pattern of distribution of the metabolites formed intracellularly;
(4) since no information was available about the cellular volumes or intracellular concentrations, all estimated parameters were based on media concentrations.

The disappearance from, or appearance into, the culture media of DZ or its metabolites was followed over 3 hr. In this way data describing eight processes were obtained. These processes were:

(1) the disappearance of DZ following DZ administration;
(2) the appearance and subsequent disappearance of NOR following DZ administration;
(3) the appearance and subsequent disappearance of TEM following DZ administration;
(4) the appearance and subsequent disappearance of OX following DZ administration;
(5) the disappearance of NOR following NOR administration;
(6) the appearance and subsequent disappearance of OX following NOR administration;
(7) the disappearance of TEM following TEM administration;
(8) the appearance and subsequent disappearance of OX following TEM administration.

Mathematical expressions for each of these functions based on the scheme presented in Fig. 1 are given in Appendix 1. Estimates of the model parameters were obtained by simultaneously fitting equations (1)–(8) to the measured media concentrations of parent substrate and metabolites, using the non-linear least squares regression program NONLIN-84, resident on a VAX 11/780, running a VMS operating system. All data points were weighted according to the reciprocal of the observed concentration, and the goodness of fit and adequacy of the model to describe the data was assessed by examination of the residual plots for each function.

RESULTS

Cellular morphology

Hepatocytes were cultured onto collagen-coated plastic six-well plates, maintained in medium buffered with sodium bicarbonate, and were adherent within 30 min, forming regular, tesselated monolayers within 3 hr. The monolayer cells were granular in appearance, with a majority of cells containing single nuclei, but only one nucleolus. Compared with rat hepatocytes, which are adherent within 2 hr, but rarely form monolayers within 5 hr, the monkey hepatocytes showed unusually rapid culturing characteristics.

The morphology of the cells was very well maintained for the whole culture period. The monolayers were initially composed of regular chords of flattened polygonal cells, and during culture the cells retained this polygonal form, with only small changes in the monolayer organisation.

No cells were observed with two nucleoli, whereas rat, dog and guinea pig cells often contained nuclei with two nucleoli, and occasionally three. About 31% of cells were binucleate, compared with rat cells in which between 26% and 32% are binucleate, and dog cells in which about 27% are binucleate.

Cellular cytochrome P-450

Table 1 compares the total cytochrome P-450 content in dog, rat, cynomolgus monkey and human in fresh (3 hr) hepatocyte cultures. Initial levels of total cytochrome P-450 in monkey hepatocytes were found to be high compared with other species. The rate of depletion of total cellular cytochrome P-450, shown in Fig. 2, was lower than that found in rat hepatocytes, so that at 6 days in culture at least 23% of total cytochrome P-450 remained in the cells,

Table 1. Comparison of the total cytochrome P-450 content of hepatocytes isolated from dog, rat, human and monkey liver, cultured for 3 hr in WME, supplemented with hydrocortisone and insulin

Species	Number of preparations	Cytochrome P-450 (pmol/10^6 hepatocytes)
Dog	4	184.3 ± 23.5
Rat	6	257.6 ± 37.3
Human	4	140.1 ± 45.7
Cynomolgus	2	430.2*

Results are given as mean ± SD.
* Mean of two determinations.

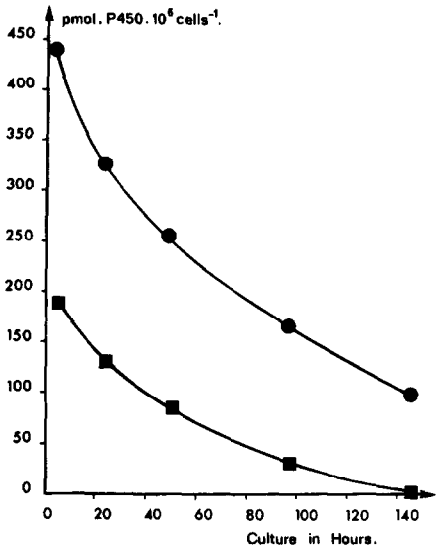

Fig. 2. Loss of total cytochrome P-450 in cynomolgus monkey hepatocytes in culture (circle), compared with that found in rat hepatocytes (square). Initial levels of cytochrome P-450/10^6 cells are high in monkey hepatocytes compared with other species in Table 2. Cells contain 94 pmol/10^6 cells after 6 days, representing better than 23% of initial cytochrome P-450.

compared with undetectable levels of cytochrome P-450 in rat cells at the same time.

Metabolism of DZ during six days in culture

The disappearance of DZ was found to be a first order process, and the rate of disappearance of DZ is shown in Fig. 3, for the intervals, 3, 24, 48, 96 and 144 hr during the culture period. Nearly complete elimination of 20 μM DZ from the culture medium was obtained during 180 min incubation on each day.

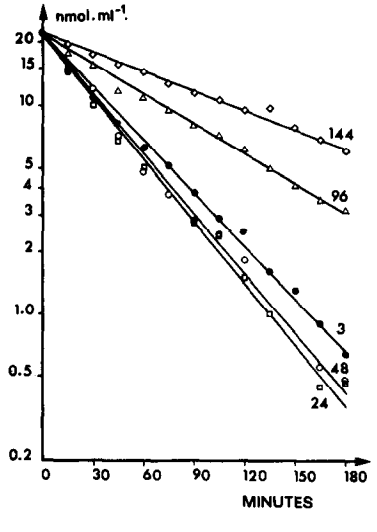

Fig. 3. Semi-log plots of the disappearance of DZ in cells cultured for 3, 24, 48, 96 and 144 hr. Disappearance is monoexponential throughout the culture period. Plots are best fit of data points.

The rates of DZ disappearance were well maintained for the initial 2 days in culture, remaining at levels comparable with those found in fresh cell culture drug incubations, but there was a decline in the rates of DZ disappearance in the subsequent 4 days.

A profile of DZ metabolism in fresh cell cultures of monkey hepatocytes is shown in Fig. 4a. It was found that NOR and TEM were major primary metabolites of DZ, with NOR representing the predominant route. The secondary metabolite, OX, was produced in significant quantities. There was no evidence of glucuronidation of any of the metabolites when samples were treated with β-glucuronidase.

Accumulation of NOR and TEM during six days in culture

The principal drug metabolizing pathways for DZ are presented in the scheme in Fig. 1, and the profiles of metabolism of DZ during 6 days in culture are shown in Fig. 4a–e. At 3 hr of culture NOR was the predominant metabolite, and accumulated throughout the incubation, achieving a maximum concentration in the medium by 90 min. The profiles of NOR accumulation obtained at 24 and 48 hr in culture were similar to those at 3 hr, but at 96 hr the extent of accumulation was reduced, and at 144 hr NOR was no longer the principal metabolite formed from DZ.

The accumulation of TEM at 3 hr in culture was relatively minor compared with the accumulation of NOR. TEM was found to accumulate for the initial 60 min of incubation, and was then observed to decline slowly during the remaining period. Similar profiles were obtained for the accumulation of TEM in hepatocytes cultured for 24 and 48 hr. At 96 hr the accumulation of TEM was considerably increased, and the time to maximum concentration was raised from 60 to 90 min. At 144 hr TEM replaced NOR as the predominant metabolite, and accumulated throughout the incubation, with no evidence of the decline obtained during the incubations with 3, 24 and 48 hr cells.

Treatment of incubation samples with β-glucuronidase did not elevate the levels of detectable TEM; TEM glucuronide was also not detectable in samples obtained from incubations with TEM as substrate.

Alterations in rate constants during culture

Rate constants k_{10}, k_{30} *and* k_{40}. Rate constants k_{10}, k_{30} and k_{40} describe the elimination of DZ, TEM and OX, respectively, via routes of metabolism which were not monitored in this study, and are summarized in Tables 2 and 3. Both k_{10} and k_{30} were found to alter in a similar manner. The values for both constants in Table 2 show that each was well maintained for the initial 48 hr, with a decline in their values in the remaining 4 days in culture.

However, the relative activities of the pathways described by these constants were dissimilar. Table 3 summarizes the relative contribution of each pathway to the metabolism of DZ, as metabolism proceeds to completion, and shows that the pathway described by k_{10} was maintained during the initial 48 hr, with a five-fold reduction in activity by 144 hr, whereas the values for constant k_{30} describing the

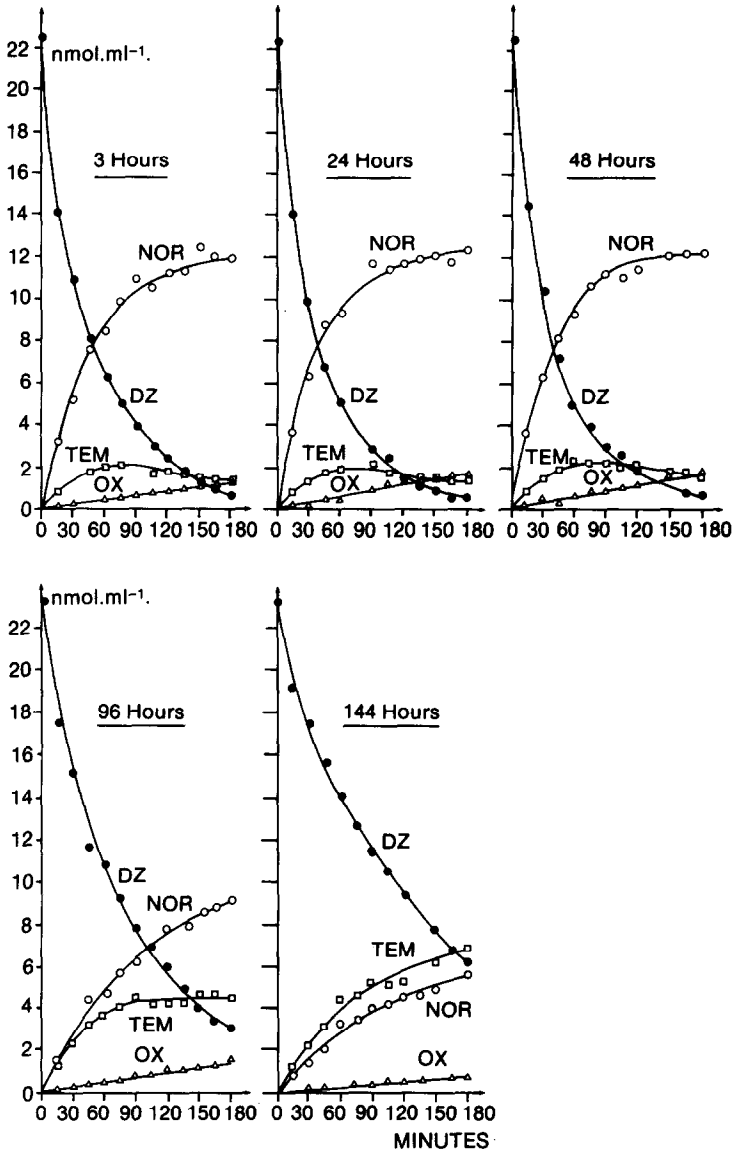

Fig. 4. Profiles of the drug metabolism of 20 μM diazepam in cynomolgus monkey hepatocytes, cultured for 6 days in WME. Drug metabolizing activities were determined at (a) 3, (b) 24, (c) 48, (d) 96 and (e) 144 hr post-isolation. Activities are well maintained for the initial 2 days, followed by a decline in the rates of DZ disappearance and significant changes in the NOR and TEM profiles, in the subsequent 4 days.

metabolism of TEM was unchanged at 96 hr, with a small reduction at 144 hr.

The rapid removal of TEM was clearly not by conjugation with glucuronic acid, so its removal may have been by C5 ring-hydroxylation [21], or diazepine ring-opening and N-deethylation [22] to form the benzophenone, or N4 oxidation [23], all of which have been reported in other species, but standards were unavailable to authenticate these routes.

Estimation of the values for rate constant k_{40} were poor, and did not permit calculation for the contribution of this pathway to the disappearance of OX.

Rate constants k_{12} *and* k_{34}. Figure 5 compares the specific changes during 6 days in culture in the rate constants of demethylation, k_{12} with k_{34}. Both rate constant profiles for the demethylation pathways were well maintained for the initial 2 days of culture followed by a rapid decline in activities representing a reduction of about 80% of initial values for k_{12} and about 50% of initial values for k_{34}, in the subsequent 4 days. The inset in Fig. 6 shows there was a similar proportional change in values of these rate constants during the culture period.

However, there were differences, shown in Table 3, in the relative activities of each demethylation pathway. The contribution of the DZ→NOR pathway to the metabolism of DZ was maintained for the initial 48 hr with a decline at 144 hr, whereas the contribution of the TEM→OX pathway to the

Table 2. Summary of the rate constants of drug metabolism of diazepam in cynomolgus monkey hepatocytes cultured for 6 days

Rate constant	Pathway	Time in culture (hr) 3	24	48	96	144
		($hr^{-1} \cdot 10^6$ cells^{-1} ± SD)				
k_{10}	DZ→?	0.644 (0.169)	0.906 (0.234)	0.921 (0.219)	0.252 (0.075)	0.076 (0.068)
k_{12}	DZ→NOR	2.640 (0.079)	3.151 (0.122)	3.030 (0.104)	1.185 (0.029)	0.613 (0.032)
k_{13}	DZ→TEM	0.755 (0.054)	0.734 (0.061)	0.842 (0.061)	0.910 (0.029)	0.791 (0.032)
k_{24}	NOR→OX	0.100 (0.029)	0.154 (0.029)	0.133 (0.029)	0.111 (0.032)	0.218 (0.058)
k_{30}	TEM→?	1.370 (0.076)	1.094 (0.065)	1.137 (0.058)	0.543 (0.058)	0.271 (0.083)
k_{34}	TEM→OX	0.457 (0.058)	0.529 (0.047)	0.421 (0.047)	0.261 (0.050)	0.237 (0.076)
k_{40}	OX→?	0.716 (0.349)	0.333 (0.280)	0.249 (0.319)	0.730 (0.691)	2.608 (1.400)

The scheme of metabolism is outlined in Fig. 1. Values in parentheses are ±1 SD of the parameter estimate.

metabolism of TEM was well maintained for 48 hr but then increased at 144 hr.

Rate constants k_{13} *and* k_{24}. The profiles of rate constants k_{13} and k_{24} for 3-hydroxylation are also shown in Fig. 5. Unlike the profiles for k_{12} and k_{34}, neither of these constants exhibited a change during culture for 6 days. The values in Table 2 are shown to be well maintained, with no alterations compared to 3 hr cultured cells.

As a consequence, the activity of the pathway DZ→TEM shown in Table 3 increased nearly three-fold during culture, but there was no alteration in the relative activity of the pathway NOR→OX.

Accumulation of OX during six days in culture

The transposition during culture of NOR and TEM as the major metabolite did not affect the accumulation of OX. The profiles of OX appearance at 3,

Table 3. Summary of the relative contribution of each pathway of metabolism to the complete metabolism of DZ as time→∞, in cynomolgus monkey hepatocytes

Rate constant Derivation	Pathway	Time in culture (hr) 3	24	48	96	144	
		Proportion of substrate metabolized by pathway					
k_{10}	DZ→?	15.9	18.9	19.2	10.7	5.1	$\frac{k_{10}}{k_{10}+k_{12}+k_{13}}$
k_{12}	DZ→NOR	65.4	65.8	63.2	50.5	41.4	$\frac{k_{12}}{k_{10}+k_{12}+k_{13}}$
k_{13}	DZ→TEM	18.7	15.3	17.6	38.8	53.4	$\frac{k_{13}}{k_{10}+k_{12}+k_{13}}$
k_{24}	NOR→OX	100	100	100	100	100	$\frac{k_{24}}{k_{24}}$
k_{30}	TEM→?	75.0	67.4	73.0	67.5	53.3	$\frac{k_{30}}{k_{30}+k_{34}}$
k_{34}	TEM→OX	25.0	32.6	27.0	32.5	46.7	$\frac{k_{34}}{k_{30}+k_{34}}$
	DZ→NOR→OX	65.4	65.8	63.2	50.5	41.4	$\%k_{12} \times \frac{k_{24}}{100}$
	DZ→TEM→OX	4.7	5.0	4.8	12.6	24.6	$\%k_{13} \times \frac{k_{34}}{100}$
	DZ→OX	70.1	70.8	68.0	63.1	66.0	$k_{12} + \frac{(\%k_{13} \times \%k_{34})}{100}$

Poor estimates of the rate constant k_{40} did not permit calculation of the relative contribution of this pathway.

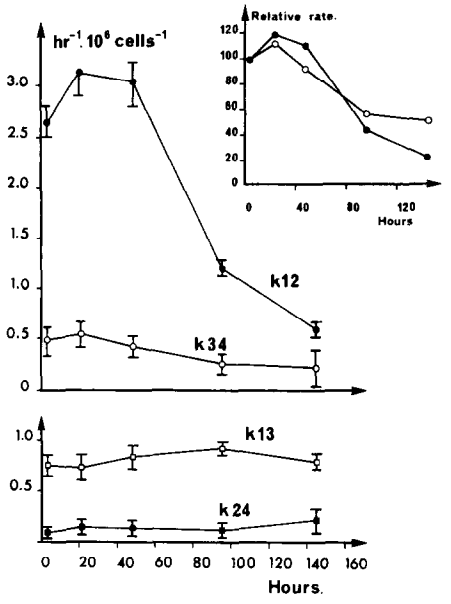

Fig. 5. Profiles of rate constants k_{12} and k_{34} (demethylation), and k_{13} and k_{24} (3-hydroxylation), determined in cynomolgus monkey hepatocytes during 6 days in culture. Points are shown with 95% confidence limits of the estimate of the parameter. There are no significant changes in the rate constants k_{13} and k_{24}. Changes in rate constants k_{12} and k_{24}, describing the demethylation activities, show similar relative profiles (inset) when expressed as a percentage of initial rate.

24, 48, 96 and 144 hr in culture were all similar. Neither of the rate constants k_{24} and k_{34}, describing the metabolism of TEM and NOR to OX, were adequately estimated from the profile data when DZ was used as the probe substrate. Therefore, specific values for rate constants k_{24} and k_{34} were obtained by introducing TEM (20 μM) and NOR (6 μM) as substrates to the monkey hepatocytes for 6 days. The metabolism of these compounds in fresh cell cultures is illustrated in Fig. 6.

This figure shows that the rate of conversion of NOR→OX was very slow. Specific estimates for k_{24}, describing this pathway and shown in Table 2, remained low for the whole period of culture, but were maintained at initial rates. There were no routes of elimination other than to OX, so the disappearance of NOR was barely detectable.

Values in Table 3 show the conversion of DZ to OX remains relatively constant during the 6-day period, whereas the relative proportions that are contributed by the routes DZ→TEM→OX and DZ→NOR→OX alter significantly. At 3 hr in culture the pathway DZ→TEM→OX contributes only 4.7% of the complete metabolism of DZ, whereas at 144 hr in culture there is a greater than five-fold increase in its contribution to 24.6%. The pathway DZ→NOR→OX alters reciprocally, contributing 65.7% at 3 hr and 41.4% at 144 hr, but this pathway reaches completion only over a long interval, since the rate of metabolism of NOR is slow.

The appearance of OX from TEM was greater than the appearance of OX from NOR. The conversion of TEM→OX was not, however, the only route by which TEM disappeared, the principal route of metabolism of TEM being by the unidentified pathway(s) described by k_{30}. TEM is also metabolized to an unidentifiable metabolite in mouse, rat and guinea-pig microsomes [23]. The pathway TEM→OX contributed only 25% of the metabolism of TEM in fresh cell cultures, but this nearly doubled by the sixth day of culture, due to a reduction in the pathway described by k_{30}.

OX was not introduced to the hepatocytes as a substrate, so the estimate of the rate constant k_{40} was inferred from the determinations made of the drug metabolism of DZ, TEM and NOR as sub-

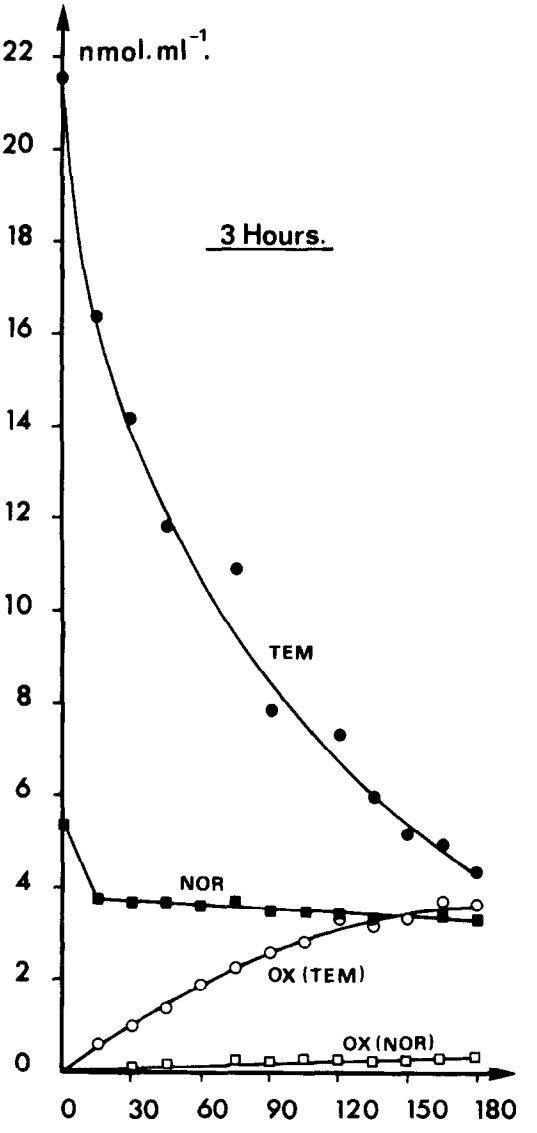

Fig. 6. Profiles of TEM (20 μM) and NOR (6 μM) metabolism in cynomolgus monkey hepatocytes after 3 hr in culture. The rate of formation of OX from NOR is much lower than the rate of formation from TEM. These profiles were observed at 3 hr (shown), 24, 48, 96 and 144 hr post-isolation (not shown), in order to determine specific values for the rate constants k_{24}, k_{34}, k_{30} and k_{40}.

strates. However, the appearance of OX remained relatively constant for the entire culture period, so the resultant changes in OX profiles with time in culture must be a complex interplay between at least three competing factors: (i) the rate of accumulation of TEM; (ii) the rate of accumulation of NOR; and (iii) the rate of disappearance of OX.

DISCUSSION

Compared with rat hepatocytes, which by 6 days have lost their regular morphology and the chords of cells become dispersed, disorganized and flattened, monkey hepatocytes show much better maintenance of morphology. These stable culturing characteristics are consistent with both their well maintained drug metabolizing functions, and cytochrome P-450 enzyme levels.

The levels of cytochrome P-450 found in monkey hepatocytes shows that monkey cells were able to retain significant levels of drug metabolizing activities even after long periods in monolayer culture.

However, the changes observed in the total cytochrome P-450 levels were not uniformly reflected by the drug metabolizing activities of these cells. Whereas cytochrome P-450 declined progressively from 3-hr values, the drug metabolizing activities of the hepatocytes towards three substrates were well maintained for 2 days, with a decline in activities only during the remaining 4 days.

Changes in the appearance of NOR during culture, shown in Fig. 4, were found to be controlled primarily by a lower activity of the demethylation enzyme(s) in the later periods of culture. Figure 3 shows no evidence of product-inhibition of DZ metabolism by NOR, although this inhibition has been reported in other species [24, 25] in which NOR was the principal metabolite. The similarities in Fig. 5 in the proportional changes of rate constants k_{12} and k_{34} for the demethylation pathways during culture strongly suggest that the same cytochrome P-450 enzyme(s) are responsible for both pathways of demethylation in cynomolgus monkey hepatocytes.

The changes in the appearance of TEM were controlled by a lower activity of the pathway described by rate constant k_{30}, but, as with NOR, also by a reduction of the activity of the demethylation enzyme(s) of the pathway TEM→OX.

During the 6 days in culture a diminishing proportion of the metabolism of TEM was due to the pathway described by rate constant k_{30}, shown in Table 3, so that at 144 hr this route had reduced from 75% to 53% and the proportion of TEM that was metabolized to OX reciprocally increased from 25% to 47%. There was also a specific decline in the values of the rate constant k_{34} for the demethylation pathway during culture, but this was less than the reduction in the values for rate constant k_{30}.

The consequence of these changes was that the accumulation of TEM increased with time in culture. This finding was initially interpreted as an induction in the enzyme activities of the 3-hydroxylation pathway DZ→TEM, but the use of TEM as a substrate in incubations at 3 (shown in Fig. 6), 24, 48, 96 and 144 hr (not shown), contradicted this interpretation. The apparent enhancement in enzyme activity was found to be a result of: (i) a reduction in its removal by pathway(s) described by rate constant k_{30}; (ii) a reduction in its removal by the pathway TEM→OX, described by rate constant k_{34}; combined with (iii) a maintained metabolism by the pathway DZ→TEM described by rate constant k_{13}.

The rate constants describing the 3-hydroxylation activities remained unaltered for the whole culture period. An absence of change in cytochrome P-450 activities is an unusual finding in cultured hepatocytes. It is rare to maintain a specific mono-oxygenase function in cultured cells without some reduction in activity. Unlike the profiles of demethylation, unaltered values of the rate constants for 3-hydroxylations do not represent evidence to suggest that these pathways are catalysed by the same cytochrome P-450 enzymes.

Therefore, considering the maintenance of the 3-hydroxylation activities for the entire 6 days of culture, in company with the observations showing DZ metabolizing activity to be unchanged during the initial 2 days in culture, this result suggests that monkey hepatocytes represent an unusually stable liver culture system.

In vitro *and* in vivo *comparisons of DZ metabolism*

The relative proportions of metabolites produced in cynomolgus monkeys *in vitro* reported here are similar to the relative proportions of those reported to be found in monkey blood [11]. This suggests that for DZ at least, the metabolites produced by monkey hepatocytes mimic those produced by hepatic metabolism in the monkey *in vivo*.

Both the hepatocyte metabolism profiles in monkey and man differ from the profiles found *in vitro* in either rat or dog cells [27].

The *in vitro* drug metabolism of DZ in human hepatocytes shows similarities with monkey hepatocytes, producing both TEM and NOR as major metabolites, and OX as a minor metabolite. These are the only metabolites that appear in human cells *in vitro*, and the appearance of each metabolite as a proportion of the disappearance of DZ are similar in cultured cells of both primates.

Despite superficial similarities in the routes of metabolism in man and the monkey, there are, however, differences in the rates of metabolism both *in vitro* and *in vivo*. In a comparison of DZ metabolism in human and monkey hepatocytes [27], the rates of disappearance of DZ (10^6 cells^{-1}) displayed a $t_{\frac{1}{2}}$ of about 25 min for monkey cells but a substantially longer $t_{\frac{1}{2}}$ of about 100 min for human hepatocytes, showing that DZ is cleared much more rapidly by monkey hepatocytes. Significantly, the ratio of the *in vitro* half lives is similar to the ratio of the half lives *in vivo*. Coutinho *et al.* [11] found that the $t_{\frac{1}{2}}$ of DZ *in vivo* for the monkey was between 4 and 6 hr, whereas Van der Kleijn *et al.* [16] found human $t_{\frac{1}{2}}$ for DZ was about 24 hr, so the four to five-fold longer differential clearance of DZ in the monkey compared to that in man was maintained *in vitro* and *in vivo*. The specific total cytochrome P-450 content of monkey hepatocytes was very much greater than the levels found in human hepatocytes, implying that monkey cells may contain higher levels of the specific enzymes responsible for DZ metabolism. It may,

therefore, be unsurprising that the clearance of DZ by the monkey is more rapid, both *in vitro* and *in vivo*.

Although some interspecies similarities exist for man and monkey between the profiles of DZ metabolism produced by hepatocytes and the profiles of DZ in blood, hepatocytes clearly cannot represent a model of all aspects of DZ disposition *in vivo*. There may be, for example, significant species differences in the biliary excretion of DZ metabolites. Nevertheless, monkey cells show significant improvements as an *in vitro* model of hepatic DZ drug metabolism compared with rat hepatocytes, with particular regard to longevity and maintenance of metabolizing activities.

In summary, monkey hepatocytes compared with rat hepatocytes show substantially better maintenance of: (i) morphology; (ii) total cytochrome P-450; and (iii) DZ drug metabolizing activities, and show considerable similarities in the *in vitro* drug metabolism of DZ to that found *in vivo* in man.

Therefore, hepatocytes isolated from the cynomolgus monkey must be considered as a very favourable model of hepatic metabolism, and more specifically, as a valuable *in vitro* model of human metabolism.

REFERENCES

1. Sirica AE and Pitot HC, Drug metabolism and effects of carcinogens in cultured hepatic cells. *Pharmacol Rev* **31**: 205, 1980.
2. Steward AR, Dannan GA, Guzelian PS and Guengerich FP, Changes in the concentration of seven forms of cytochrome P450 in primary cultures of adult rat hepatocytes. *Molec Pharmacol* **27**: 125–132, 1984.
3. Michalopoulos G, Sattler GL and Pitot HC, Maintenance of microsomal cytochromes b5 and P-450 in primary cultures of parenchymal liver cells on collagen membranes. *Life Sci* **18**: 1139–1144, 1976.
4. Holme JA, Soderlund E and Dybing E, Drug metabolism activities of isolated rat hepatocytes in monolayer culture. *Acta Pharmacol Toxicol* **52**: 348–356, 1983.
5. Grant MH, Melvin MAL, Shaw P, Melvin WT and Burke MD, Studies on the maintenance of cytochromes P-450 and b_5, monooxygenases and cytochrome reductases in primary cultures of rat hepatocytes. *FEBS Lett* **190**: 99–103, 1985.
6. Guillouzo A, Beaune P, Gascoin MN, Begue JM, Campion JP, Guengerich FP and Guguen-Guillouzo C, Maintenance of cytochrome P-450 in cultured adult human hepatocytes. *Biochem Pharmacol* **34**: 2991–2995, 1985.
7. Decad GM, Hsieh DPH and Byard JL, Maintenance of cytochrome P450 and metabolism of aflatoxin-B1 in primary hepatocyte cultures. *Biochem Biophys Res Commun* **78**: 279–287, 1977.
8. Paine AJ, Williams LJ and Legg RF, Apparent maintenance of cytochrome P450 by nicotinamide in primary cultures of rat hepatocytes. *Life Sci* **24**: 2185–2192, 1979.
9. Lebreton LP, Daveau M, Hiron M, Fontaine M, Biou D, Gilbert D and Guguen-Guillouzo C, Long-term biosynthesis of complement component C3 and α-1 acid glycoprotein by adult rat hepatocytes in a coculture system with an epithelial liver cell type. *Biochem J* **235**: 421–427, 1986.
10. Guguen-Guillouzo C, Clement B, Baffet G, Beaumont C, Morel-Chany E, Glaise D and Guillouzo A, Maintenance and reversibility of active albumin secretion by adult rat hepatocytes co-cultured with another liver epithelial cell type. *Exp Cell Res* **143**: 47–54, 1983.
11. Coutinho CB, Cheripko JA, Carbone JJ, Manning JE and Boff E, Behavioural changes in primates and diazepam metabolism. *Xenobiotica* **3**: 681–690, 1973.
12. Vree TB, Baards AM, Hekster YA, Van der Kleijn E and O'Reilly WJ, Simultaneous determination of diazepam and its metabolites *N*-desmethyl diazepam, oxydiazepam and oxazepam in plasma and urine of man and dog by means of high pressure liquid chromatography. *J Chromatogr* **162**: 605–614, 1979.
13. Ohnhaus EE, Park BK, Colombo JP and Heizmann P, The effect of enzyme induction on diazepam metabolism in man. *Br J Clin Pharmacol* **8**: 557–563, 1979.
14. Chenery RJ, Ayrton A, Oldham HG, Standring P and Norman SJ, Diazepam metabolism in cultured hepatocytes from rat, rabbit, dog, guinea pig and man. *Drug Metab Disp* **15**: 312–318, 1987.
15. Klotz U, Antonin K-H and Bieck PR, *J Pharmacol Exp Ther* **199**: 67–73, 1976.
16. Van der Kleijn E, Possum JM, Muskens ETJM and Rijntjes NVM, Pharmacokinetics of diazepam in dogs, mice and humans. *Acta Pharmacol Toxicol* **3**: 109–127, 1971.
17. Boxenbaum H, Comparative pharmacokinetics of benzodiazepines in dog and man. *J Pharmacokin Biopharm* **10**: 411–425, 1982.
18. Strom SC, Jirtle RA, Jones RS, Irons, DL, McLain JR and Michalopoulos G, Isolation, culture and transplantation of human hepatocytes. *J Natn Cancer Inst* **68**: 771–778, 1982.
19. Warner M, Lamaca MV and Neims AH, Chromatographic and electrophoretic heterogeneity of the cytochromes P450 solubilised from untreated rat liver. *Drug Metab Disp* **6**: 353–362, 1978.
20. Omura R and Sato R, The carbon monoxide binding pigment of liver microsomes. *J Biol Chem* **239**: 2379–2385, 1964.
21. Ruelius HW, Lee JM and Alburn HE, Metabolism of diazepam in dogs: transformation to oxazepam. *Arch Biochem Biophys* **111**: 376–380, 1965.
22. Schwartz MA and Postma E, Metabolism of diazepam *in vitro*. *Biochem Pharmacol* **17**: 2443–2449, 1968.
23. Garrattini S, Marcucci F and Mussini E, Benzodiazepine metabolism *in vitro*. *Drug Metab Rev* **1**: 291–309, 1972.
24. Klotz U and Reitmann I, Clearance of diazepam can be impaired by its major metabolite desmethyl diazepam. *Eur J Clin Pharmacol* **21**: 161–163, 1981.
25. Savenije-Chapel EM, Bast A and Noordhoek J, Inhibition of diazepam metabolism in microsomal and perfused liver preparations of the rat by *n*-desmethyl diazepam, *N*-methyl oxazepam and oxazepam. *Eur J Drug Metab Pharmacokinet* **10**: 15–20, 1985.
26. Andrews SM and Griffiths LA, The metabolism and disposition of [2-^{14}C]diazepam in the streptozotocin-diabetic rat. *Xenobiotica* **14**: 751–760, 1984.
27. Seddon T, Michelle I and Chenery RJ, Comparative drug metabolism of diazepam in hepatocytes isolated from man, rat, monkey and dog. *Biochem Pharmacol* **38**: 1657–1665, 1989.

APPENDIX 1

From the scheme in Fig. 1 the following system of differential equations can be derived:

$$\frac{dA_1}{dt} = -A_1 . K_1$$

$$\frac{dA_2}{dt} = A_1 . k_{12} - A_2 . k_{24}$$

$$\frac{dA_3}{dt} = A_1 . k_{13} - A_3 . K_3$$

$$\frac{dA_4}{dt} = A_2 . k_{24} + A_3 . k_{34} - A_4 . k_{40}.$$

Let a_n be the Laplace transform of A_n and let the initial conditions of A_1 be D and $A_2 = A_3 = A_4 = 0$.

Then, converting to Laplace transforms yields:

$$\begin{aligned} sa_1 - D &= -K_1 . a_1 \\ sa_2 &= k_{12} . a_1 - k_{24} . a_2 \\ sa_3 &= k_{13} . a_1 - k_3 . a_3 \\ sa_4 &= k_{24} . a_2 + k_{34} . a_3 - k_{40} . a_4. \end{aligned}$$

Rearranging these equations gives:

$$\begin{aligned} D &= (s+K_1) . a_1 \\ 0 &= -k_{12} . a_1 + (s+k_{24}) . a_2 \\ 0 &= -k_{13} . a_1 + (s+K_3) . a_3 \\ 0 &= -k_{24} . a_2 - k_{34} . a_3 + (2+k_{40}) . a_4. \end{aligned}$$

The determinant, Δ, of the system is given by:

$$\Delta = (s+K_1)(s+k_{24})(s+K_3)(s+k_{40}).$$

Solutions for the amounts in compartments 1–4 can now be obtained as follows:

$$\begin{aligned} a_1 &= \frac{\begin{vmatrix} D & 0 & 0 & 0 \\ 0 & s+k_{24} & 0 & 0 \\ 0 & 0 & s+K_3 & 0 \\ 0 & -k_{24} & -k_{34} & s+k_{40} \end{vmatrix}}{\Delta} \\ &= \frac{D . (s+k_{24})(s+k_3)(s+k_{40})}{(s+K_1)(s+k_{24})(s+K_3)(s+k_{40})} \\ &= \frac{D}{(s+K_1)}. \end{aligned}$$

$$A_1 = D . e^{-K_1 . t}. \tag{1}$$

In a similar manner, values for A_2, A_3 and A_4 following dosing into A_1 can be derived. These equations are given below

$$A_2 = \frac{D . k_{12}}{k_{24} - K_1}(e^{-K_1 . t} - e^{-k_{24} . t}) \tag{2}$$

$$A_3 = \frac{D . k_{13}}{K_3 - K_1}(e^{-K_1 . t} - e^{-K_3 . t}) \tag{3}$$

$$\begin{aligned} A_4 = D . k_{13} . k_{34} &\left(\frac{1}{(K_3 - K_1)(k_{40} - K_1)} e^{-K_1 . t}\right. \\ &+ \frac{1}{(K_1 - k_{31})(k_{40} - K_3)} e^{-K_3 . t} \\ &\left. + \frac{1}{(K_1 - k_{40})(K_3 - k_{40})} e^{-k_{40} . t}\right) \\ + D . k_{24} . k_{12} &\left(\frac{1}{(K_{24} - K_1)(k_{40} - K_1)} e^{-K_1 . t}\right. \\ &+ \frac{1}{(K_1 - k_{24})(k_{40} - k_{24})} e^{-k_{24} . t} \\ &\left. + \frac{1}{(K_1 - k_{40})(k_{24} - k_{40})} e^{-k_{40} . t}\right). \end{aligned} \tag{4}$$

Equations (1)–(4) represent amounts following administration into compartment 1 (DZ). Similar equations can be derived for administration into compartments 2 (NOR) and 3 (TEM).

Following administration into 2, the equations for the amounts in compartments 2 and 4 are:

$$A_2 = D . e^{-k_{24} . t} \tag{5}$$

$$A_4 = \frac{D . k_{24}}{(k_{24} - k_{40})}(e^{-k_{40} . t} - e^{-k_{24} . t}). \tag{6}$$

Similarly the expressions for the amounts in compartments 3 and 4 following administration to compartment 3 are given by:

$$A_3 = D . e^{-K_3 . t} \tag{7}$$

$$A_4 = \frac{D . k_{34}}{(K_3 - k_{40})}(e^{-k_{40} . t} - e^{-K_3 . t}). \tag{8}$$